


# One-Pot Synthesis, Photoluminescence, and Electrocatalytic Properties of Subnanometer-Sized Copper Clusters

Wentao Wei,<sup>†,§</sup> Yizhong Lu,<sup>†,§</sup> Wei Chen,<sup>\*,†</sup> and Shaowei Chen<sup>\*,#</sup>

<sup>†</sup>State Key Laboratory of Electroanalytical Chemistry, Changchun Institute of Applied Chemistry, Chinese Academy of Sciences, Changchun 130022, Jilin, China

<sup>‡</sup>Graduate School of the Chinese Academy of Sciences, Beijing 100039, China

<sup>#</sup>Department of Chemistry and Biochemistry, University of California, 1156 High Street, Santa Cruz, California 95064, United States

 Supporting Information

**ABSTRACT:** Subnanometer-sized copper nanoclusters were prepared by a one-pot procedure based on wet chemical reduction. The structural characteristics of the 2-mercapto-5-*n*-propylpyrimidine-protected nanoclusters, Cu<sub>*n*</sub> (*n* ≤ 8), were determined by mass spectrometry. The Cu nanoclusters displayed apparent luminescence, with dual emissions at 425 and 593 nm, with quantum yields of 3.5 and 0.9%, respectively, and high electrocatalytic activity in the electroreduction of oxygen.

Metal nanoclusters have attracted considerable attention because of their unique size-dependent optical and electronic properties that differ substantially from those of the corresponding atoms and bulk materials, and thus exhibit great potentials as unique functional building blocks in a wide range of applications such as optoelectronic nanodevices, biosensors, nanoelectronics, and novel catalysts.<sup>1,2</sup> For metal nanoparticles with sizes comparable to the Fermi wavelength of an electron, strong photoluminescence can be observed due to the presence of discrete energy levels and energy band-gap structures. In recent years, extensive studies have been focused on luminescent Au and Ag nanoclusters.<sup>3–10</sup> These studies show that the energy structures of metal nanoparticles exhibit strong size dependency. For example, when the dimensions of alkanethiolate-protected gold nanoparticles decrease to the (sub)nanometer regime, the electronic structure exhibits a transition from bulk-like to molecule-like behaviors,<sup>11</sup> as reflected by, for instance, the blue shift of the nanoparticle luminescence from near-IR/red to blue emission.<sup>12–15</sup> However, despite extensive research progress of luminescent Au and Ag nanoclusters, studies focusing on the synthesis and optical properties of other nanoclusters such as copper are still scarce primarily because of the difficulty in preparing highly stable and extremely tiny particles. For instance, copper clusters with diameters smaller than 4–6 nm have been synthesized within dendrimer templates,<sup>16,17</sup> whereas copper nanoparticles synthesized by traditional wet chemical reduction methods are typically larger than 10 nm in diameter, and only recently were copper clusters, Cu<sub>*n*</sub>, with *n* ≤ 13, synthesized by electrochemical and microemulsion techniques.<sup>18,19</sup> Herein, we report the synthesis of stable Cu<sub>*n*</sub> (*n* ≤ 8) nanoclusters by a simple one-pot chemical reduction method by using 2-mercapto-5-*n*-propylpyrimidine

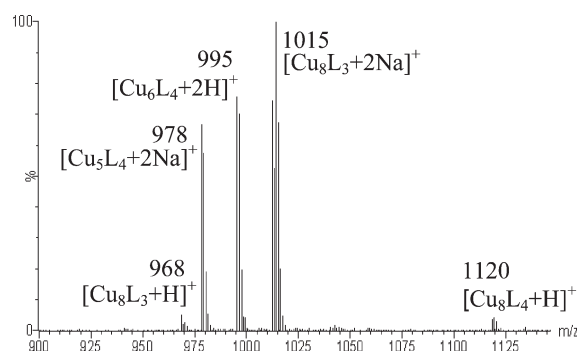


**Figure 1.** Representative ESI mass spectrum of a copper cluster sample detected in the positive-ion mode.

(MPP) as the protecting ligand. The resulting nanoclusters exhibited interesting photoluminescence, with dual emissions at 423 and 593 nm, with quantum yields of 3.5 and 0.9%, respectively, and, more interestingly, high catalytic activity in the electroreduction of oxygen.

In this study, copper nanoclusters, soluble in nonpolar solvents such as toluene, hexane, and chloroform, were prepared by a facile one-phase process. In a typical synthesis, copper(II) nitrate and tetra-*n*-octylammonium bromide were co-dissolved in alcohol. The solution was stirred at 80 °C for 30 min and then cooled in ice water. MPP and sodium borohydride in ethanol were then added successively into the reaction mixture. The resultant products were obtained by centrifugation and purification (more details of the experimental procedure are included in the Supporting Information (SI)). For subnanometer-sized metal clusters, conventional (high-resolution) transmission electron microscopy is not a reliable technique in the evaluation of cluster size distribution. In contrast, mass spectrometry techniques, such as electrospray ionization mass spectrometry (ESI-MS) and matrix-assisted laser desorption ionization mass spectrometry, have been proved to be powerful tools for cluster size analysis.<sup>7,20</sup> Thus, the chemical composition of the Cu nanoclusters was first analyzed with positive-ion ESI-MS. Figure 1 shows the ESI-MS spectrum in the high-mass range. The highest mass peak, *m/z* ≈ 1120, can be assigned to the Cu clusters with a composition of Cu<sub>8</sub>L<sub>4</sub> (L = C<sub>7</sub>H<sub>9</sub>N<sub>2</sub>S), whereas those in the lower mass range may be ascribed to the fragments of

**Received:** October 15, 2010

**Published:** January 31, 2011

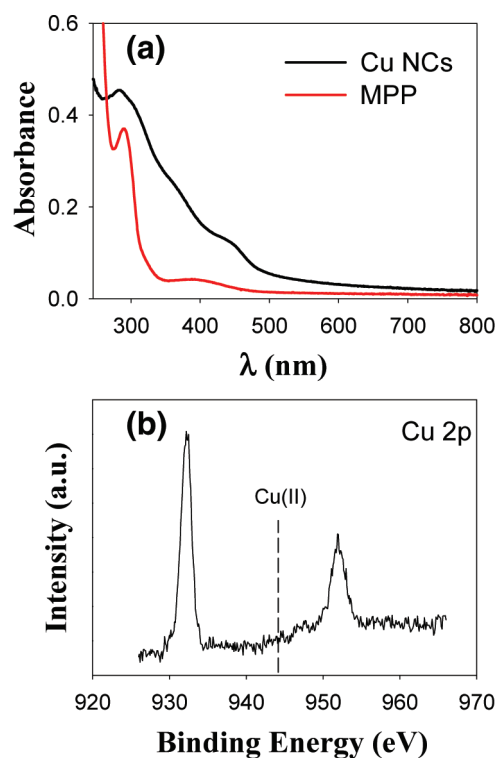


**Figure 2.** (a) UV-vis absorption spectra of the Cu nanoclusters and monomeric MPP in  $\text{CHCl}_3$ . (b) X-ray photoelectron spectrum of Cu 2p electrons in Cu nanoclusters; the dashed line shows the binding energy of Cu(II) 2p electrons.

$\text{Cu}_8\text{L}_3$  ( $m/z = 1015$ ),  $\text{Cu}_6\text{L}_4$  (995),  $\text{Cu}_5\text{L}_4$  (978),  $\text{Cu}_8\text{L}_3$  (968), and  $\text{Cu}_5\text{L}_1$  (470) (SI, Figure S1). Among these,  $\text{Cu}_8$  clusters are the dominant Cu-containing components in the colloid solution. Note that the experimental MS profiles are consistent with the simulated isotopic patterns (as manifested in SI, Figure S2). Previously, extensive theoretical studies have predicted the existence of stable  $\text{Cu}_n$  clusters with  $n = 1-9^{21,22}$  and  $\text{Cu}_{13}$  as the smallest copper cluster with a three-dimensional closed-shell structure.<sup>18,19</sup> To the best of our knowledge, this is the first report of wet chemical synthesis of Cu clusters with less than eight atoms.

It is widely accepted that metal nanoclusters with core diameters smaller than 1 nm exhibit one or more absorption peaks, in contrast to the surface plasmon resonance (SPR) band observed with larger particles, due to the molecule-like characters of the electronic energy structure. Figure 2a shows the UV-vis absorption profiles of the Cu nanoclusters (black curve) as well as the monomeric MPP ligands (red curve). Three well-defined absorption peaks can be observed with the Cu-MPP nanoclusters at 285, 364, and 443 nm, which are ascribed to the interband electronic transitions of the Cu clusters due to the discrete energy levels. Note that these optical features are clearly different from the characteristic SPR band of large Cu nanoparticles at 560–600 nm<sup>23–25</sup> or those of the MPP ligands. The powder X-ray diffraction (XRD) pattern is shown in the SI, Figure S3. The broadening of the diffraction peaks into the baseline is consistent with the tiny size of the Cu clusters.

The oxidation state of Cu was then investigated by X-ray photoelectron spectroscopy (XPS) measurements. It should be noted that in previous studies where Cu nanoclusters were prepared by the electrochemical method,<sup>18</sup> XPS measurements

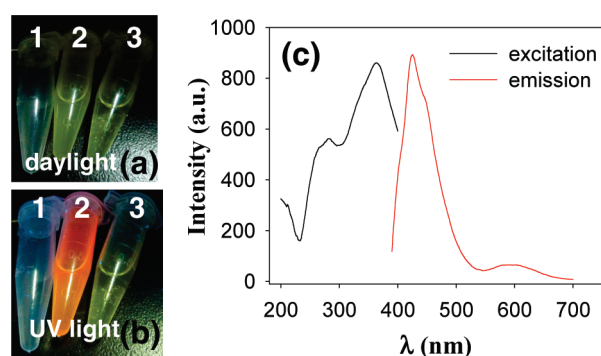


**Figure 3.** Photographs of the samples under (a) daylight and (b) UV light: (1) empty tube; (2) Cu clusters in  $\text{CHCl}_3$ ; (3) MPP in  $\text{CHCl}_3$ . (c) Excitation (black curve,  $\lambda_{\text{em}} = 425$  nm) and emission (red curve,  $\lambda_{\text{ex}} = 364$  nm) spectra of the copper nanoclusters in  $\text{CHCl}_3$ .

indicated a substantial presence of Cu(II) in the sample, which was removed only after sputtering with  $\text{Ar}^+$  ions. In the present study, two peaks were observed at 932.3 and 952.0 eV (Figure 2b), which are assigned to the binding energies of the  $2p_{3/2}$  and  $2p_{1/2}$  electrons of Cu(0), and no feature for Cu(II) electrons was observed, suggesting the lack of significant oxidation of the Cu nanoclusters. Nevertheless, it is known that the  $2p_{3/2}$  binding energy of Cu(0) is only  $\sim 0.1$  eV away from that of Cu(I) species. Therefore, the valence state of the obtained Cu clusters most likely lies between 0 and +1. This is not surprising since the Cu atoms in such tiny clusters are expected to be positive because of charge transfer in the  $\text{Cu}-\text{SC}_7\text{H}_9\text{N}_2$  bonds. The XPS spectra of other elements are shown in the SI, Figure S4. The binding energy of S  $2p_{3/2}$  (162.7 eV) compares very well with the typical value of chemisorbed S species.<sup>26</sup> Further structural characterizations were carried out by FTIR measurements, and the results show that the Cu nanoclusters were passivated by MPP through Cu-S bonding interactions (SI, Figure S5). Notably, the broad peak observed with the MPP ligands at  $2525\text{ cm}^{-1}$  can be assigned to the S-H stretching vibrational mode, which disappeared completely with the Cu nanoclusters, indicating the cleavage of the S-H bond and the binding of the  $\text{C}_7\text{H}_9\text{N}_2\text{S}$  fragment onto the Cu surface through Cu-S bonds. Energy dispersive X-ray analysis (not shown) also shows the presence of Cu and S in the sample. It should be noted that in previous syntheses by the electrochemical and micro-emulsion techniques,<sup>18,19</sup> the Cu nanoclusters were electrostatically or sterically stabilized by bulky ionic surfactants, such as (cationic) tetrabutylammonium nitrate and (anionic) sodium dodecyl sulfate, and because of the nonbonding interactions between the nanoparticle cores and surface protecting ligands, it is challenging to further functionalize the nanoparticles. By contrast, in the present procedure, the Cu nanoclusters were stabilized by the chemical bonding interactions of copper with MPP, where the enhanced stability renders it possible to further functionalize and engineer the particle structures and properties in a reliable fashion.

Interestingly, the solution of the Cu nanoclusters is golden yellow under ambient daylight but exhibits an orange color when irradiated with a UV lamp ( $\lambda = 365$  nm), as shown in the optical photographs of sample 2 in Figure 3a,b, in sharp contrast to the monomeric MPP ligands (sample 3) or the sample container (sample 1). Figure 3c depicts the photoluminescence spectra of the Cu nanoclusters. The excitation spectrum (black curve)

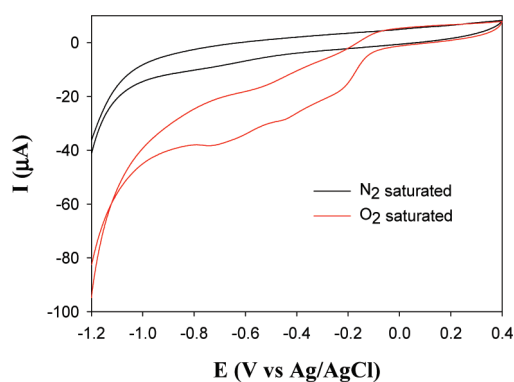


**Figure 4.** Cyclic voltammograms of Cu-NCs/GC electrode in 0.1 M KOH saturated with  $N_2$  (black curve) or  $O_2$  (red curve). Potential scan rate, 0.1 V/s.

shows two maxima at 283 and 364 nm, which are similar to the absorption peaks in Figure 2b. Under excitation at 364 nm, strong blue and yellow luminescence with emission maxima at 425 and 593 nm can be clearly observed (red curve), where the respective quantum yield at ambient temperature in air was evaluated to be 3.5% and 0.9%, corresponding to an overall quantum yield of about 4.4%. Such a dual luminescence phenomenon has also been observed in previous studies of glutathione-protected  $Au_{25}$  nanoclusters and gold(I) complex.<sup>12,27,28</sup> For the Au clusters, Whetten et al.<sup>12</sup> assigned the high-energy luminescence to the interband transition from excited states in the sp-band to d-band, whereas the low-energy luminescence was assigned to the intraband HOMO–LUMO transition within the sp band. For gold complexes,<sup>27,28</sup> the high-energy luminescence was typically assigned to the metal-perturbed intraligand phosphorescence and the low-energy luminescence to the triplet states of a ligand-to-metal charge-transfer character that mixes with metal-centered states modified by Au–Au interactions. However, in previous studies where the Cu nanoclusters were synthesized by other methods,<sup>18,19</sup> only one luminescence band was observed in the blue region. Since the photoluminescence of metal clusters is size-dependent, the two emissions shown in Figure 3 may originate either from the same clusters, as discussed above, or from Cu clusters of different sizes. Figure S6 (SI) depicts the excitation spectra for the two emissions, where it can be seen that the excitation peaks are almost identical at 364 nm, suggesting that the emissions at 593 and 425 nm most probably arose from the same active cluster centers. Further studies based on quantum calculations are desired to unravel the mechanistic origin of the dual luminescence observed above with the Cu nanoclusters.

Recently, copper complexes have been found to exhibit significant electrocatalytic activity for oxygen reduction reactions (ORR).<sup>29,30</sup> Here, the electrocatalytic activity of Cu nanoclusters as cathode catalysts for ORR was examined by electrochemical measurements, with the Cu clusters deposited onto a glassy carbon electrode (referred to as Cu-NCs/GC). Figure 4 shows the cyclic voltammograms of Cu-NCs/GC in 0.1 M KOH saturated with either  $N_2$  or  $O_2$  at a potential scan rate of 0.1 V/s. It can be seen that, in the  $N_2$ -saturated solution, only a featureless voltammetric profile was observed within the potential range of  $-1.2$  to  $+0.4$  V. By contrast, when the electrolyte solution was saturated with  $O_2$ , obvious reduction currents emerged, suggesting the electrocatalytic activity of the Cu nanoclusters for oxygen reduction. Although a quantitative

comparison of the reduction currents cannot be reliably made at the moment with literature results, the onset potential of  $O_2$  reduction ( $-0.07$  V, Figure 4) was found to be highly comparable to those observed with  $Au_{11}$  clusters ( $-0.08$  V)<sup>20</sup> and some commercial Pt catalysts,<sup>31</sup> suggesting that copper nanoclusters might serve as effective non-platinum electrocatalysts for fuel cell electrochemistry.<sup>20,31–34</sup> In addition, repeated cycling of potentials yielded almost identical voltammograms, indicative of the structural stability of the Cu nanoclusters during electrocatalysis.

In conclusion, we demonstrated that MPP-protected copper nanoclusters,  $Cu_n$  with  $n \leq 8$ , could be successfully synthesized with a simple method based on one-pot wet chemical reduction. The cluster composition was characterized by electrospray ionization mass spectrometry. This is the first time that stable copper nanoclusters with less than eight atoms in the core were synthesized. The clusters exhibited interesting dual luminescence, with emission maxima at 425 and 593 nm, and thus might be exploited as a novel fluorophore. The synthesized Cu nanoclusters also showed a high catalytic activity for oxygen reduction. Such low-cost electrocatalyst might serve as effective cathode catalysts in alkaline fuel cells. Ongoing work is focused on the investigation of the crystal structure and size-controlled synthesis of Cu nanoclusters and the size-dependent electrocatalytic activity for oxygen reduction, and results will be reported in due course.

## ■ ASSOCIATED CONTENT

**S Supporting Information.** Detailed experimental procedures, ESI-MS, XPS, XRD, and FTIR data, and photoluminescence measurements of the copper nanoclusters. This material is available free of charge via the Internet at <http://pubs.acs.org>.

## ■ AUTHOR INFORMATION

### Corresponding Author

weichen@ciac.jl.cn; shaowei@ucsc.edu

### Author Contributions

<sup>5</sup>These authors contributed equally to this work.

## ■ ACKNOWLEDGMENT

This work was supported by the National Natural Science Foundation of China (No. 21043013) and CIAC (W.C.). S.C. acknowledges support by the National Science Foundation (CHE-0718170 and CHE-1012258).

## ■ REFERENCES

- (1) Valden, M.; Lai, X.; Goodman, D. W. *Science* **1998**, *281*, 1647–1650.
- (2) Elghanian, R.; Storhoff, J. J.; Mucic, R. C.; Letsinger, R. L.; Mirkin, C. A. *Science* **1997**, *277*, 1078–1081.
- (3) Zheng, J.; Petty, J. T.; Dickson, R. M. *J. Am. Chem. Soc.* **2003**, *125*, 7780–7781.
- (4) Bigioni, T. P.; Whetten, R. L.; Dag, O. *J. Phys. Chem. B* **2000**, *104*, 6983–6986.
- (5) Zheng, J.; Ding, Y.; Tian, B. Z.; Wang, Z. L.; Zhuang, X. W. *J. Am. Chem. Soc.* **2008**, *130*, 10472–10473.
- (6) Zheng, J.; Zhang, C. W.; Dickson, R. M. *Phys. Rev. Lett.* **2004**, *93*, 077402.
- (7) Wu, Z. K.; Lanni, E.; Chen, W. Q.; Bier, M. E.; Ly, D.; Jin, R. C. *J. Am. Chem. Soc.* **2009**, *131*, 16672–16673.

- (8) Zhu, M.; Lanni, E.; Garg, N.; Bier, M. E.; Jin, R. *J. Am. Chem. Soc.* **2008**, *130*, 1138–1139.
- (9) Mrudula, K. V.; Rao, T. U. B.; Pradeep, T. *J. Mater. Chem.* **2009**, *19*, 4335–4342.
- (10) Rao, T. U. B.; Pradeep, T. *Angew. Chem., Int. Ed.* **2010**, *49*, 3925–3929.
- (11) Chen, S. W.; Ingram, R. S.; Hostetler, M. J.; Pietron, J. J.; Murray, R. W.; Schaaff, T. G.; Khoury, J. T.; Alvarez, M. M.; Whetten, R. L. *Science* **1998**, *280*, 2098–2101.
- (12) Link, S.; Beeby, A.; FitzGerald, S.; El-Sayed, M. A.; Schaaff, T. G.; Whetten, R. L. *J. Phys. Chem. B* **2002**, *106*, 3410–3415.
- (13) Huang, T.; Murray, R. W. *J. Phys. Chem. B* **2001**, *105*, 12498–12502.
- (14) Wilcoxon, J. P.; Martin, J. E.; Parsapour, F.; Wiedenman, B.; Kelley, D. F. *J. Chem. Phys.* **1998**, *108*, 9137–9143.
- (15) Zheng, J.; Nicovich, P. R.; Dickson, R. M. *Annu. Rev. Phys. Chem.* **2007**, *58*, 409–431.
- (16) Balogh, L.; Tomalia, D. A. *J. Am. Chem. Soc.* **1998**, *120*, 7355–7356.
- (17) Zhao, M. Q.; Sun, L.; Crooks, R. M. *J. Am. Chem. Soc.* **1998**, *120*, 4877–4878.
- (18) Vilar-Vidal, N.; Blanco, M. C.; Lopez-Quintela, M. A.; Rivas, J.; Serra, C. *J. Phys. Chem. C* **2010**, *114*, 15924–15930.
- (19) Vazquez-Vazquez, C.; Banobre-Lopez, M.; Mitra, A.; Lopez-Quintela, M. A.; Rivas, J. *Langmuir* **2009**, *25*, 8208–8216.
- (20) Chen, W.; Chen, S. W. *Angew. Chem., Int. Ed.* **2009**, *48*, 4386–4389.
- (21) Cao, Z. X.; Wang, Y. J.; Zhu, J.; Wu, W.; Zhang, Q. *J. Phys. Chem. B* **2002**, *106*, 9649–9654.
- (22) Poater, A.; Duran, M.; Jaque, P.; Toro-Labbe, A.; Sola, M. *J. Phys. Chem. B* **2006**, *110*, 6526–6536.
- (23) Lisiecki, I.; Pileni, M. P. *J. Phys. Chem.* **1995**, *99*, 5077–5082.
- (24) Mott, D.; Galkowski, J.; Wang, L. Y.; Luo, J.; Zhong, C. *J. Langmuir* **2007**, *23*, 5740–5745.
- (25) Salzemann, C.; Lisiecki, I.; Brioude, A.; Urban, J.; Pileni, M. P. *J. Phys. Chem. B* **2004**, *108*, 13242–13248.
- (26) Bensebaa, F.; Ellis, T. H.; Kruus, E.; Voicu, R.; Zhou, Y. *Langmuir* **1998**, *14*, 6579–6587.
- (27) Yam, V. W. W.; Cheng, E. C. C.; Cheung, K. K. *Angew. Chem., Int. Ed.* **1999**, *38*, 197–199.
- (28) Yam, V. W. W.; Cheng, E. C. C.; Zhou, Z. Y. *Angew. Chem., Int. Ed.* **2000**, *39*, 1683–1684.
- (29) Thorum, M. S.; Yadav, J.; Gewirth, A. A. *Angew. Chem., Int. Ed.* **2009**, *48*, 165–167.
- (30) Brushett, F. R.; Thorum, M. S.; Lioutas, N. S.; Naughton, M. S.; Tornow, C.; Jhong, H. R.; Gewirth, A. A.; Kenis, P. J. A. *J. Am. Chem. Soc.* **2010**, *132*, 12185–12187.
- (31) Gong, K. P.; Du, F.; Xia, Z. H.; Durstock, M.; Dai, L. M. *Science* **2009**, *323*, 760–764.
- (32) Tang, W.; Lin, H. F.; Kleiman-Shwarsstein, A.; Stucky, G. D.; McFarland, E. W. *J. Phys. Chem. C* **2008**, *112*, 10515–10519.
- (33) Campbell, F. W.; Belding, S. R.; Baron, R.; Xiao, L.; Compton, R. G. *J. Phys. Chem. C* **2009**, *113*, 9053–9062.
- (34) Herzing, A. A.; Kiely, C. J.; Carley, A. F.; Landon, P.; Hutchings, G. J. *Science* **2008**, *321*, 1331–1335.